

The maize *brown midrib2 (bm2)* gene encodes a methylenetetrahydrofolate reductase that contributes to lignin accumulation

Ho Man Tang^{1,†}, Sanzhen Liu^{2,*,*}, Sarah Hill-Skinner², Wei Wu^{2,3,§}, Danielle Reed^{1,§}, Cheng-Ting Yeh², Dan Nettleton^{3,4} and Patrick S. Schnable^{1,2,3,*}

¹Department of Genetics, Development and Cell Biology, Iowa State University, Ames, IA 50011, USA,

²Department of Agronomy, Iowa State University, 2035 Roy J. Carver Co-Lab, Ames, IA 50011-3650, USA,

³Center for Plant Genomics, Iowa State University, 2035 Roy J. Carver Co-Lab, Ames, IA 50011-3650, USA, and

⁴Department of Statistics, Iowa State University, 2115 Snedecor, Ames, IA 50011, USA

Received 29 January 2013; revised 31 October 2013; accepted 20 November 2013; published online 26 November 2013.

*For correspondence (e-mails liu3zhen@ksu.edu (SL) or schnable@iastate.edu (PSS)).

Ho Man Tang and Sanzhen Liu contributed equally to this work.

†Present address: Center for Cell Dynamics, Department of Biological Chemistry, Johns Hopkins University School of Medicine, Baltimore, MD 21205, USA.

‡Present address: Department of Plant Pathology, Kansas State University, Manhattan, KS 66506, USA.

§Present address: Pioneer Hi-Bred International Inc., Johnston, IA 50131, USA.

SUMMARY

The midribs of maize *brown midrib (bm)* mutants exhibit a reddish-brown color associated with reductions in lignin concentration and alterations in lignin composition. Here, we report the mapping, cloning, and functional and biochemical analyses of the *bm2* gene. The *bm2* gene was mapped to a small region of chromosome 1 that contains a putative methylenetetrahydrofolate reductase (MTHFR) gene, which is down-regulated in *bm2* mutant plants. Analyses of multiple *Mu*-induced *bm2-Mu* mutant alleles confirmed that this constitutively expressed gene is *bm2*. Yeast complementation experiments and a previously published biochemical characterization show that the *bm2* gene encodes a functional MTHFR. Quantitative RT-PCR analyses demonstrated that the *bm2* mutants accumulate substantially reduced levels of *bm2* transcript. Alteration of MTHFR function is expected to influence accumulation of the methyl donor *S*-adenosyl-L-methionine (SAM). Because SAM is consumed by two methyltransferases in the lignin pathway (Ye *et al.*, 1994), the finding that *bm2* encodes a functional MTHFR is consistent with its lignin phenotype. Consistent with this functional assignment of *bm2*, the expression patterns of genes in a variety of SAM-dependent or -related pathways, including lignin biosynthesis, are altered in the *bm2* mutant. Biochemical assays confirmed that *bm2* mutants accumulate reduced levels of lignin with altered composition compared to wild-type. Hence, this study demonstrates a role for MTHFR in lignin biosynthesis.

Keywords: *Zea mays*, *brown midrib*, lignin, methylenetetrahydrofolate, *S*-adenosyl-L-methionine.

INTRODUCTION

Lignin is a heterogeneous aromatic polymer that is a major component of cell walls. It plays a critical role in the structural integrity of vascular plants (Sarkanen and Ludwig, 1971). In lignified tissues, lignin is heavily cross-linked with cellulose and hemicelluloses to provide protection and strength, and also increases the resistance of biomass to enzymatic digestion by ruminants, bacteria and fungi (Sarkanen and Ludwig, 1971). This high level of resistance to enzymatic digestion has a negative effect on forage quality and cellulosic biofuel production (Ragauskas *et al.*, 2006; Penning *et al.*, 2009), reducing the efficiency by

which lignocellulosic biomass is converted to biofuels such as ethanol (Fu *et al.*, 2011). In contrast, a reduction in lignin content significantly improves digestibility and animal performance. Reduced lignin content of livestock feed also reduces animal waste (Jung and Vogel, 1986). Therefore, an understanding of the mechanisms that regulate lignin accumulation has the potential to provide important insights that may be used to improve the quality of biomass and forage crops.

Maize (*Zea mays* ssp. *mays* L.) is a widely grown and highly productive food, feed and biofuel crop (Doebley

et al., 2006; Tang et al., 2010). *Brown midrib* (*bm*) mutants are characterized by the reddish-brown color of their leaf midribs (Sattler et al., 2010). The *bm* phenotype of maize was first reported over 80 years ago (Jorgenson, 1931), and it is now clear that this phenotype is associated with reduced lignin concentrations (Grand et al., 1985; Cherney et al., 1991; Sattler et al., 2010). To date, six *bm* mutants have been identified. The *bm1*, *bm2*, *bm3*, *bm4*, *bm5* and *bm6* loci are located on chromosomes 5, 1, 4, 9, 5 and 2, respectively (Chen et al., 2012; Lawrence et al., 2005; Sattler et al., 2010). The *bm1* and *bm3* genes encode cinnamyl alcohol dehydrogenase (CAD) (Barrière et al., 2013; Halpin et al., 1998) and caffeic acid *O*-methyltransferase (COMT) (Vignols et al., 1995), respectively. Both play key roles in lignin biosynthesis. The roles of the other four *bm* genes in lignin biosynthesis are not clear. Therefore, cloning the remaining *bm* genes is expected to provide insights into the regulation of lignin biosynthesis.

In this study, a candidate *bm2* gene was identified via a map-based approach. Analyses of multiple independent *Mutator* transposon insertion alleles confirmed that the candidate gene is indeed *bm2*. A yeast complementation experiment demonstrated that, as predicted based on its sequence, *bm2* encodes a functional methylenetetrahydrofolate reductase (MTHFR, EC 1.5.1.20). Alteration of MTHFR function is expected to influence accumulation of the methyl donor *S*-adenosyl-L-methionine (SAM). An RNA-Seq experiment demonstrated that the *bm2* mutation significantly affects expression of genes involved in several SAM-related metabolic pathways, including the lignin/phenylpropanoid pathway, ethylene and jasmonate metabolism, and glutathione *S*-transferase (GST) genes. Collectively, these results demonstrate a role for MTHFR in the lignin biosynthetic pathway.

RESULTS

Characterization of the *bm2* mutant phenotype and lignin content in various tissues

The *bm2* mutant was originally identified by its brown pigmentation in the leaf midrib (Neuffer et al., 1968), a description that is consistent with our observations of the *bm2-ref* allele. In the genetic backgrounds used in this study, *bm2-ref* mutants first exhibit a reddish-brown pigmentation of the leaf midrib beginning at the 6–8-leaf stage, approximately 27 days after planting (Figure 1a). The reddish-brown pigmentation observed on both the adaxial and abaxial surfaces of mutant leaves was not observed in non-mutant siblings (Figure 1a).

In addition to these biochemical assays, *bm2* mutant samples from various tissues were stained with phloroglucinol, which detects lignin (Wardrop, 1971). In B73 and non-mutant sibling maize, the midrib, epidermis and tissues around vascular bundles stain red with phloroglucinol,

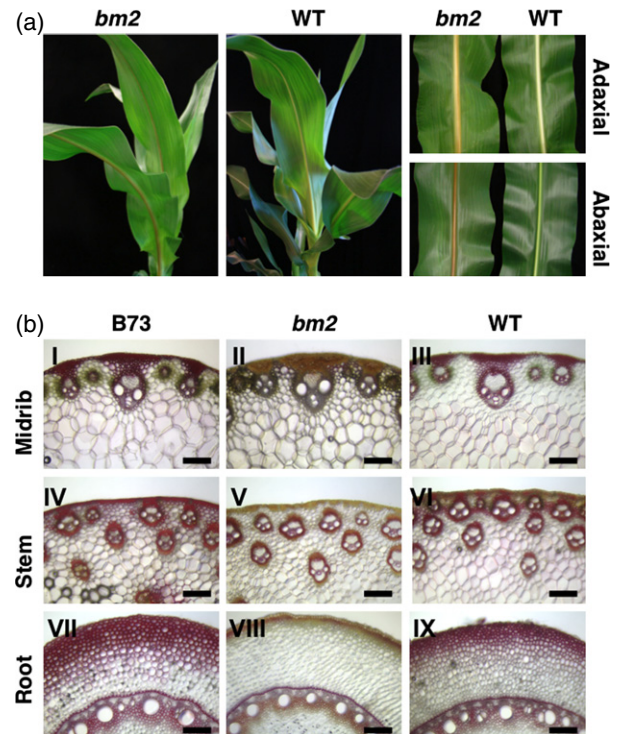


Figure 1. Characterization of the *bm2-ref* mutant.

(a) The left panels show greenhouse-grown *bm2* mutant (*bm2-ref*) and non-mutant sibling/wild-type (WT) maize.

The right panels show abaxial and adaxial views of the midribs of *bm2* mutant and WT maize.

(b) Histochemical staining of lignin of tissue sections from B73, *bm2* mutant and WT maize. Sections of midrib (I–III), stem (IV–VI) and root (VII–IX) were taken from B73 (I, IV, VII), *bm2* mutant (II, V, VIII) and non-mutant sibling (III, VI, IX) maize that had been stained with phloroglucinol. Scale bars = 100 μ m.

thereby demonstrating lignification of these tissues. However, in the *bm2* mutant, these tissues stain only weakly. Although there are no observable alterations in the anatomy of stems and roots associated with the *bm2* mutant, significant differences in phloroglucinol staining were detected in these tissues. In B73 and non-mutant sibling stems and roots, strong phloroglucinol staining was detected at xylem vessels and epidermis, whereas *bm2* mutant tissues exhibited reduced staining. These phloroglucinol staining results are consistent with previous reports (Vermerris and Boon, 2001; Marita et al., 2003; Sattler et al., 2010) indicating that lignin levels are lower in the *bm2* mutant compared to non-mutant controls (Figure 1b).

Mutant *bm2* plants have also been reported to accumulate reduced lignin concentrations and levels of G-lignin (Vermerris and Boon, 2001; Marita et al., 2003; Sattler et al., 2010). However, the reports are inconsistent with respect to the effect of the *bm2* mutation on concentrations of S-lignin (Vermerris and Boon, 2001; Marita et al., 2003; Saballos et al., 2009; Sattler et al., 2010; Vermerris et al., 2010). In some instances, S-lignin concentrations have been found to

be lower in the *bm2* mutant (Vermerris *et al.*, 2010), but have been reported to be unchanged or even elevated in other cases (Vermerris and Boon, 2001; Marita *et al.*, 2003; Barriere *et al.*, 2004; Sattler *et al.*, 2010). Due to this ambiguity, we re-analyzed the lignin in *bm2* mutants.

Classically, due to the interest in utilizing stover for feed, biochemical assays of lignin have classically been performed at or around the stage at which maize is harvested for silage (i.e. after anthesis, but before maturity). We were interested to determine whether lignin characteristics changed between this stage and senescence. We therefore determined Klason lignin and the lignin composition of *bm2* mutant and non-mutant sibling (wild-type) stalks collected directly post-anthesis (PA) and post-senescence (PS). Consistent with literature, we found that mutant PA stalks accumulated only approximately 93% of the Klason lignin of wild-type siblings. Mutant PS samples exhibited similar reductions in lignin concentrations. Both mutant and wild-type PS samples accumulated more Klason lignin (approximately 112%) than the corresponding PA samples, showing that lignin continues to accumulate in stalks after flowering.

Lignin is composed of at least three hydroxycinnamyl alcohol subunits (the monolignols *p*-coumaryl, coniferyl and sinapyl alcohol), resulting in hydroxyphenyl (H), guaiacyl (G) and syringyl (S) types of lignin, respectively (Whetten and Sederoff, 1995; Bonawitz and Chapple, 2010). In maize, H-lignin represents only a small fraction (approximately 2%) of total lignin (Barrière *et al.*, 2007). Hence, the monolignol composition of lignin was measured as the μmol of S- or G-lignin per gram of dry stalk tissue. We found that the ratio of S- to G-lignin was elevated in the *bm2* mutant compared to wild-type siblings at both stages of development. In agreement with the Klason lignin data, the absolute amounts of both S- and G-lignin were lower, on average, in mutant samples relative to wild-type and PA samples relative to PS samples (Table 1). These results are consistent with a role for the *bm2* gene in lignin biosynthesis.

Mapping the *bm2* gene

The *bm2* gene was previously mapped to the long arm of chromosome 1 (www.maizegdb.org) (Neuffer *et al.*, 1968;

Lawrence *et al.*, 2005). To map the *bm2* gene to a higher resolution, we used a modification of bulked segregant analysis called bulked segregant RNA-Seq (BSR-Seq), which makes use of the quantitative feature of RNA-Seq (Liu *et al.*, 2012). Briefly, RNA-Seq reads are generated from pools of *bm2* mutants and non-mutant (wild-type) siblings. Because of the digital nature of next-generation sequencing data, it is possible to perform *de novo* SNP discovery and quantitatively genotype bulked samples using the same RNA-Seq data.

To generate a *bm2* mapping population, a *bm2-ref* mutant plant was crossed to the non-mutant inbred line B73. A *bm2-ref* heterozygous individual was self-pollinated to generate an F₂ segregating population. From this segregating population, tissue samples from siblings exhibiting the mutant and non-mutant phenotypes were combined into two separate pools and subjected to RNA-Seq (Experimental procedures). RNA-Seq reads were trimmed and aligned to the B73 reference genome (Schnable *et al.*, 2009). In total, 46 289 SNPs were identified and used for the BSR-Seq analysis.

Via the BSR-Seq analysis, the *bm2* gene was located to an approximately 2 Mb region of chromosome 1 from 289–291 Mb (Figure 2), which contains 83 genes in the filtered gene set (Table S1). Subsequently, 41 individuals from an F₂ mapping population ($n = 537$) that contained recombination events within this 2 Mb interval were identified using two flanking SNP markers (Experimental procedures). Twelve additional SNP markers (Table S2) located within the 2 Mb interval were used to narrow down the *bm2* mapping interval to an approximately 0.5 Mb region that contains 47 genes from the working gene set (Table S3). Only eight of these 47 genes are members of the more confidently defined 'filtered gene set' (Table S4). Of the 47 genes, only one (GRMZM2G347056, which is not a member of the filtered gene set) exhibited significant down-regulation in mutant versus wild-type sibling samples as assayed via the RNA-Seq experiments described below (Appendix S1). This *bm2* candidate gene encodes a putative methylenetetrahydrofolate reductase (MTHFR).

A BLASTP (blast.ncbi.nlm.nih.gov/Blast.cgi) search of a variety of plants demonstrated that many dicots contain

Table 1 Lignin characteristics of wild-type and *bm2* mutant siblings at various developmental stages

Stage	Genotype	Klason lignin (g g ⁻¹ dry weight)	S/G	S ($\mu\text{mol g}^{-1}$ dry weight)	G ($\mu\text{mol g}^{-1}$ dry weight)	S + G ($\mu\text{mol g}^{-1}$ dry weight)
PA	Wild-type	0.162 ± 0.014	1.24 ± 0.06	1037 ± 140	843 ± 157	1880 ± 297
	Mutant	0.151 ± 0.010	1.74 ± 0.23	896 ± 59	518 ± 34	1414 ± 25
PS	Wild-type	0.182 ± 0.008	1.70 ± 0.18	1402 ± 52	832 ± 121	2233 ± 233
	Mutant	0.170 ± 0.021	1.97 ± 0.23	1054 ± 45	539 ± 85	1593 ± 130

Each genotype represents the mean of two technical replicates and two biological replicates. One biological replicate is a single whole stalk. PA, post-anthesis (approximately 2 months old); PS, post-senescence (approximately 5 months old).

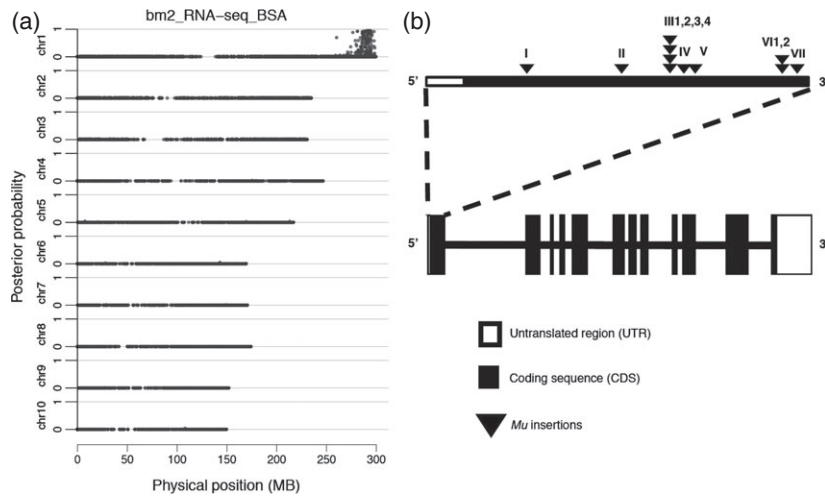


Figure 2. *bm2* mapping and cloning.

(a) Mapping of *bm2* via BSR-Seq. Each dot represents one SNP site. The x axis indicates the physical position (Mb) of each SNP site on the indicated chromosomes. The y axis indicates the probability of complete linkage between an indicated SNP site and the *bm2* gene. The mapping result is consistent with the reported position of the *bm2* gene (as downloaded from MaizeGDB, www.maizegdb.org).

(b) Transposon insertion sites in *bm2-Mu* alleles, including (I) *bm2-Mu-10-7090B*, (II) *bm2-Mu-10-7073G*, (III1) *bm2-Mu-10-7067E-2*, (III2) *bm2-Mu-10-7067A*, (III3) *bm2-Mu-10-7067E-1*, (III4) *bm2-Mu-10-7067F*, (IV) *bm2-Mu-10-7065G*, (V) *bm2-Mu-10-7061A*, (VI1) *bm2-Mu-10-7049D*, (VI2) *bm2-Mu-10-7084F*, and (VII) *bm2-Mu-10-7045B*. The corresponding histochemical staining of lignin of tissue sections is shown in Figure S2. *Mu* insertions are indicated by triangles.

two apparently full-length MTHFR homologs, while grasses contain only a single apparently full-length MTHFR homolog (Figure S11).

However, maize contains a second protein (AFW67208) encoded by the GRMZM2G034278 gene that exhibits 96% identity to the *bm2*-encoded protein, but with only 52% coverage. We initially hypothesized that this partial MTHFR gene may be part of a Pack-MULE, but it is not included among those identified in the B73 genome (RefGen_v1) by Jiang *et al.* (2011).

Confirmation that the *bm2* and MTHFR-encoding genes are one and the same

To confirm that the candidate gene is the *bm2* gene, additional *bm2* mutant alleles were identified via a direct *Mu* transposon tagging experiment. A population of plants derived from a cross of plants carrying an active *Mu* transposon system with plants homozygous for the *bm2-ref* allele was screened for *Mu*-induced *bm2* mutant alleles (Experimental procedures). After screening 147 500 individuals, 11 plants were identified that exhibited the characteristic reddish-brown midribs of *bm2* mutants (Figure S2). These individuals were PCR-screened using a *Mu*-specific primer together with *mthfr*-specific primers (Experimental procedures). *Mu* insertions were identified in the MTHFR-encoding gene in each of the 11 identified mutants, including a total of seven unique *Mu* insertion sites (Figure 2 and Figure S1). Although some mutants have identical *Mu* insertion sites (as has been observed previously, Dietrich *et al.*, 2002), the design of our tagging experiment

ensured that each mutant arose via an independent event. Homozygous *bm2-Mu* lines were generated for each of the 11 mutants (Experimental procedures), and phloroglucinol staining indicated that these individuals accumulate reduced levels of lignin (Figures S2 and S3), demonstrating that the MTHFR-encoding gene is indeed the *bm2* gene.

The *bm2* gene is expressed constitutively

To test whether the *bm2* gene is specifically expressed in lignified tissues, we used the online tool, qTeller (qteller.com), to visualize its expression in a variety of organs at multiple stages of development (Figure S12). From this analysis, it is clear that the *bm2* gene is expressed in almost all tissues assayed, including some that are not lignified (e.g. ovules, primordial apices and endosperm).

The accumulation of *bm2* transcripts is dramatically reduced in *bm2* mutants

The RNA-Seq data from the BSR-Seq experiment indicated that the *bm2* gene is down-regulated in midribs of the *bm2-ref* mutant relative to non-mutant sibling controls (Appendix S1). RT-PCR and quantitative RT-PCR performed on multiple biological replicates confirmed this pattern of differential expression in *bm2-ref* and *bm2-Mu* mutants compared to wild-type (B73 and non-mutant siblings). This down-regulation occurs in multiple tissues, including leaf, stem, root and midrib (Figure 3a,b and Figure S1D).

Quantitative RT-PCR analysis of lines homozygous for each of our 11 *bm2-Mu* lines was performed on RNA

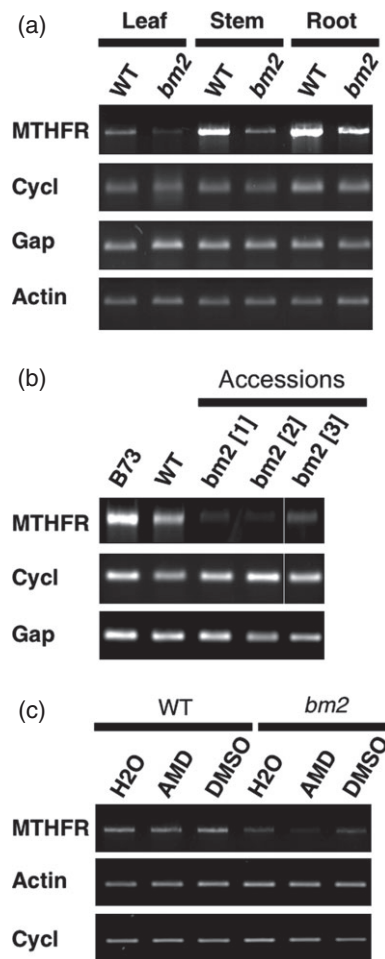


Figure 3. MTHFR gene mRNA accumulation in *bm2* mutants. (a) RT-PCR gel analysis of the accumulation of MTHFR gene mRNA in various tissues, including leaf, midrib and root of wild-type (WT) and *bm2-ref* (*bm2*, Schnable Lab accession number Ac3247 and stock number 11B-418-1) plants. (b) RT-PCR gel analysis of the accumulation of MTHFR gene mRNA in *bm2* mutants in four distinct genetic backgrounds: *bm2* [1] (Schnable Lab accession number Ac3247 and stock number 10B-611-16); *bm2* [2] (Schnable Lab accession number Ac3247 and stock number 11-1051); *bm2* [3] (Schnable Lab accession number Ac3244 and stock number 11-1049), B73 (Schnable Lab accession number Ac660 and stock number 10B-613-9) and non-mutant (WT, Schnable Lab accession number Ac3247 and stock number 10-611-50). (c) Accumulation of MTHFR gene mRNA in midribs of wild-type and *bm2-ref* (Schnable Lab accession number Ac3247 and stock number 11-1051) after or without treatment with actinomycin D (AMD, 50 $\mu\text{g ml}^{-1}$, 12 h). Incubation of the corresponding tissues in water or DMSO served as mock experiments. Accumulation of mRNA for actin, cyclin or GAP served as a loading control.

extracted from two biological replicates of each genotype. The results showed that *bm2* transcript accumulation was reduced to as little as 5% of B73 expression in several of the *bm2* mutants and to less than 10% in all but two of the mutants (Figure S1D). These results are in line with our expectations based on the fact that all of the *bm2-Mu*

alleles contain *Mu* insertions within the coding region of the *bm2* gene.

The RT-PCR products from the *bm2-ref* allele were sequenced and compared to the B73 reference genome. Seven polymorphisms were identified in the *bm2-ref* allele relative to the B73 reference genome (Figure S4). One is a synonymous mutation in the coding region; the other six polymorphisms are located in the 3' UTR (Figure S4). We hypothesized that the reduced accumulation of *bm2* mRNA in the *bm2-ref* mutant may be the result of the 3' UTR polymorphisms because the 3' UTR plays a critical role in RNA stability (Gutierrez *et al.*, 1999; Millevoi and Vagner, 2010).

To test the stability of the *bm2* mRNA from non-mutant (wild-type) and *bm2-ref* mutant siblings, the corresponding midrib tissues were exposed to the transcription inhibitor actinomycin D (Sawicki and Godman, 1972; Experimental procedures). After a 12 h incubation of the tissues in the presence of actinomycin D, the level of *bm2* mRNA in the *bm2-ref* tissue was reduced, while the level of the non-mutant control remained similar to its original level (Figure 3c). This finding demonstrates that the transcripts from the *bm2-ref* allele are less stable than non-mutant transcripts and are consistent with our hypothesis that the polymorphisms in the 3' UTR in the *bm2-ref* allele reduce the stability of the MTHFR-encoding gene mRNA.

The maize *bm2* cDNA complements *MET11* knockout yeast

The maize *bm2* gene shares 40% amino acid identity and 59% similarity with the yeast *MET11* gene, which encodes a functional homolog of the human MTHFR protein (Figure S5). MTHFR catalyzes the conversion of 5,10-methylenetetrahydrofolate to 5-methyltetrahydrofolate, a co-substrate for homocysteine re-methylation to methionine (Goyette *et al.*, 1994; Vickers *et al.*, 2006). Yeast lacking the endogenous *MET11* gene are unable to grow on methionine-free medium (Shan *et al.*, 1999). To test the hypothesis that the maize *bm2* gene encodes a functional MTHFR enzyme, an *MET11* knockout strain (*met11*) of yeast was used to test whether expression of the maize *bm2* gene rescues *met11* yeast. As expected, wild-type yeast (*MET11*) but not the *met11* strain grew in the absence of methionine (Figure 4). Further, consistent with a previous report (Shan *et al.*, 1999), expression of the human MTHFR-encoding gene rescues *met11* yeast in the presence of galactose, which induces expression of the human MTHFR-encoding gene construct (Figure 4). Significantly, when under the control of a galactose-inducible promoter, the non-mutant *bm2* cDNA also rescued *met11* yeast in the presence of galactose, but not in the presence of glucose, which inhibits expression of *bm2* in this construct (Figure 4). This finding demonstrates that the *bm2* gene encodes a functional MTHFR.

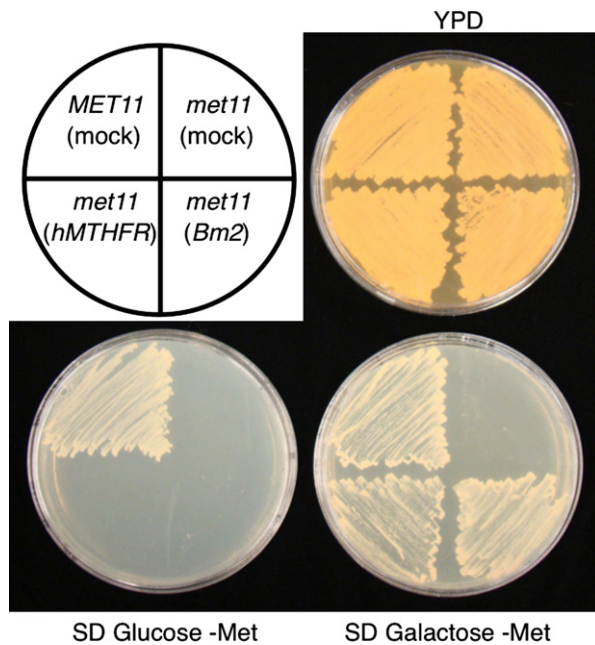


Figure 4. Yeast complementation assay. Growth of yeast strains on plates containing yeast extract/peptone/dextrose (YPD, control), SD glucose -Met (control) or SD galactose -Met (to induce expression of the plasmid insert). *MET11* (mock), wild-type yeast transformed with plasmid without insert; *met11* (mock), *MET11* knockout yeast transformed with empty plasmid; *met11* (*Bm2*), *MET11* knockout yeast transformed with plasmid containing maize *mthfr*; *met11* (*hMTHFR*), *MET11* knockout yeast transformed with plasmid containing human *MTHFR* (positive control of the complementation assay).

Transcriptomic analysis of a *bm2* mutant

We performed two independent RNA-Seq experiments. These experiments differed in terms of the age of plants harvested, the number of replicates analyzed, and the statistical cut-offs used to define differentially expressed genes. The first experiment (#1) included a single replication using 26-day-old midrib tissue. The second experiment (#2) included two biological replications of 38-day-old tissue (Tables S5–S7). In an effort to minimize false discovery, more stringent cut-offs were used in experiment #1 compared to the second experiment (#2) because the former did not include a biological replication.

RNA-Seq experiment #1 identified 369 significantly differentially expressed genes with a >2-fold change between *bm2* mutants and their wild-type siblings; of these, 242 were up-regulated and 127 were down-regulated relative to wild-type. RNA-Seq experiment #2 identified 3313 differentially expressed genes (Figures S6–S8 and Appendix S1). Nearly 90% ($n = 323$) of the 369 differentially expressed genes from RNA-Seq experiment #1 (which lacked a biological replication) were also detected in RNA-Seq experiment #2 (Figure S9). The following functional analysis is based on the results of RNA-Seq experiment #2

that included two biological replicates. A pathway enrichment analysis of the 3313 differentially expressed genes from RNA-Seq experiment #2 revealed statistically significant over-representation of the following functional categories: lignin/phenylpropanoid (Figure S10), hormone ethylene, hormone jasmonate and glutathione *S*-transferase (GST) gene families, and cytochrome P450s (Table S8).

The *p*-coumaryl (H), coniferyl (G) and sinapyl (S) alcohol subunits of lignin are synthesized by enzymes in the phenylpropanoid pathway, including phenylalanine ammonia lyase (PAL), hydroxycinnamoyl CoA:shikimate hydroxycinnamoyl transferase (HCT), 4-coumarate:CoA ligase (4CL), cinnamyl alcohol dehydrogenase (CAD), cinnamoyl CoA reductase (CCR), caffeoyl CoA 3-*O*-methyltransferase (CCoAOMT) and caffeic acid 3-*O*-methyltransferase (COMT) (Lewis and Yamamoto, 1990; Tamasloukht *et al.*, 2011). In RNA-Seq experiment #2, 41 of 109 genes involved in the phenylpropanoid pathway are significantly differentially expressed between the *bm2* mutants and wild-type sibling controls (Table 2). The majority of these significantly differentially expressed genes were up-regulated in *bm2* mutants as compared to wild-type sibling controls. These included genes that encode members of the PAL, cinnamate-4-hydroxylase (C4H), HCT, CAD and 4CL families. Three CAD-encoding genes (GRMZM2G090980, GRMZM2G443445 and AC234163.1_FG002), an HCT-encoding gene (GRMZM2G089698) and a 4CL-encoding gene (GRMZM2G048522) were each up-regulated at least 16-fold in the *bm2* mutant relative to the wild-type (Table 2). Interestingly, the cloned *bm1* gene (GRMZM5G844562) that encodes CAD was down-regulated in the *bm2* mutant.

The *bm2*-encoded MTHFR enzyme is involved in the metabolism of methionine, a precursor of the methyl donor *S*-adenosyl-L-methionine (SAM). Two SAM-dependent methyltransferases, caffeoyl CoA 3-*O*-methyltransferase (CCoAOMT) and caffeic acid 3-*O*-methyltransferase (COMT), participate in the phenylpropanoid pathway. However, among nine genes that are annotated in MapMan (Thimm *et al.*, 2004) as encoding these two methyltransferases, only one (GRMZM2G099363) was significantly down-regulated in the *bm2* mutant relative to the wild-type siblings, and this exhibited only a small decrease (0.65-fold). Similarly, the previous cloned COMT-encoding gene *bm3* (AC196475.3_FG004) was not significantly differentially expressed in our RNA-Seq experiments with a false discovery rate of $\leq 5\%$ (Table S9). Two peroxidase genes (AC205413.4_FG001 and GRMZM2G126261) involved in lignin assembly were significantly up-regulated in the *bm2* mutant. One of them, AC205413.4_FG001, was up-regulated >16-fold (Appendix S1). Consistent with the role of peroxidases in polymerization of monolignols into lignin (Quiroga *et al.*, 2000), the peroxidase family was enriched among the differentially expressed genes.

Table 2 Differentially expressed genes in the phenylpropanoid pathway in the *bm2* mutant as compared to wild-type siblings

Sort order	Gene	MapMan annotation	log ₂ fold change (mutant/wild-type)	P value	Adjusted P value
1	GRMZM2G160541	PAL	-1	1.61E-03	1.73E-02
2	GRMZM2G081582	PAL	0.86	2.73E-04	5.36E-03
3	GRMZM2G063917	PAL	1.19	3.05E-03	2.58E-02
4	GRMZM2G334660	PAL	1.77	1.12E-03	1.36E-02
5	GRMZM2G089698	HCT	5.54	5.58E-07	9.96E-05
6	AC210173.4_FG005	F5H	-2.09	1.59E-04	3.74E-03
7	GRMZM2G099363	CCoAOMT	-0.62	7.51E-03	4.50E-02
8	GRMZM5G844562	CAD (<i>bm1</i>)	-0.7	7.89E-03	4.64E-02
9	GRMZM2G090980	CAD	4.12	3.78E-06	3.31E-04
10	GRMZM2G443445	CAD	10.27	2.85E-09	5.78E-06
11	AC234163.1_FG002	CAD	31.9	8.70E-07	1.26E-04
12	GRMZM2G139874	C4H	1.78	1.18E-04	3.11E-03
13	GRMZM2G147245	C4H	4.22	2.65E-05	1.14E-03
14	GRMZM2G012233	4CL	-0.95	3.89E-03	2.98E-02
15	GRMZM2G048522	4CL	2.42	1.33E-03	1.53E-02
16	GRMZM2G051005	No annotation	-1.79	5.67E-04	8.77E-03
17	GRMZM2G156004	No annotation	-1.66	1.37E-05	7.68E-04
18	GRMZM2G158083	No annotation	-0.98	1.76E-04	3.99E-03
19	GRMZM2G179703	No annotation	-0.97	1.90E-03	1.92E-02
20	GRMZM2G409724	No annotation	-0.87	3.41E-03	2.76E-02
21	GRMZM2G017557	No annotation	-0.78	4.98E-03	3.47E-02
22	GRMZM2G108714	No annotation	-0.77	2.07E-03	2.02E-02
23	GRMZM2G094017	No annotation	0.74	3.16E-04	5.94E-03
24	AC217947.4_FG002	No annotation	1.03	2.19E-03	2.10E-02
25	GRMZM2G060210	No annotation	1.11	2.24E-03	2.13E-02
26	GRMZM2G138624	No annotation	1.2	1.36E-03	1.55E-02
27	GRMZM2G035023	No annotation	1.63	3.43E-04	6.23E-03
28	GRMZM2G147503	No annotation	1.96	2.85E-04	5.54E-03
29	GRMZM2G165192	No annotation	2.05	2.18E-04	4.61E-03
30	GRMZM2G061806	No annotation	2.72	1.09E-04	2.93E-03
31	GRMZM2G408458	No annotation	3.17	2.43E-05	1.09E-03
32	GRMZM2G127418	No annotation	3.94	6.26E-04	9.32E-03
33	GRMZM2G015793	No annotation	4.14	4.52E-06	3.71E-04
34	GRMZM2G124815	No annotation	4.67	5.78E-07	1.01E-04
35	GRMZM2G089698	No annotation	5.54	5.58E-07	9.96E-05
36	GRMZM2G127251	No annotation	6.63	3.08E-06	2.90E-04
37	GRMZM2G362298	No annotation	7.69	2.08E-05	9.91E-04
38	GRMZM2G311036	No annotation	7.84	5.74E-06	4.25E-04
39	GRMZM2G114918	No annotation	19.77	4.43E-05	1.61E-03
40	GRMZM2G023325	No annotation	20.45	7.48E-05	2.25E-03
41	GRMZM2G336824	No annotation	33.71	3.45E-05	1.37E-03

DISCUSSION

Plants homozygous for *bm2* mutations exhibit reddish-brown pigmentation of their leaf midribs, and also accumulate reduced lignin levels; the lignin that does accumulate has an altered composition as compared to non-mutant maize (Vermerris and Boon, 2001; Marita *et al.*, 2003; Sattler *et al.*, 2010). Here, we describe molecular characterization of the cloned *bm2* gene. Analysis of multiple independent *Mu*-induced alleles of the *bm2* gene demonstrated that the putative MTHFR-encoding gene located in this interval that is down-regulated in the *bm2* mutant is indeed the *bm2* gene. Complementation studies performed in yeast demonstrate that the *bm2* gene encodes a

functional MTHFR. In addition, a previous study (Roje *et al.*, 1999) showed that expression in MTHFR-deficient yeast strains of a maize cDNA derived from what we now know is the *bm2* gene displayed both forward and reverse MTHFR enzyme activities. This observation, in combination with our quantitative RT-PCR analysis of 11 *bm2-Mu* lines, suggests that the *bm2* mutants have, at most, greatly reduced levels of MTHFR activity.

Survival of *bm2* mutants

MTHFR plays a critical role in the biosynthesis of methionine (Goyette *et al.*, 1994; Vickers *et al.*, 2006), an essential sulfur-containing amino acid. Apart from its nutritional

importance and central role in the initiation of mRNA translation, methionine indirectly regulates a variety of important cellular processes, including the biosynthesis of DNA, RNA, protein, lipid and hormones (Amir, 2010). Based on the essential role of this enzyme in yeast, it is predicted that knockout mutants of *bm2* would be lethal. However, plants homozygous for the *bm2-ref* allele or any of the *Mu* insertion alleles are viable. Because methionine is an essential amino acid, the survival of these *bm2* mutants suggests that they accumulate sufficient amounts of methionine. In our RNA-Seq analyses of *bm2* mutants, genes associated with protein synthesis are under-represented among the differentially expressed genes, consistent with the hypothesis that protein synthesis is not disrupted in *bm2* mutants (Table S8 and Appendix S1). There are at least two possible explanations for the viability of the *bm2* mutants. First, the *bm2* mutant alleles may be leaky. However, including both the reference and *Mu* insertion alleles, 12 *bm2* mutant alleles have been identified; all are homozygous viable. It is unlikely that all of these are leaky, particularly as each of the 11 *Mu*-induced alleles contains a transposon insert in the coding region. If the partial *bm2* paralog GRMZM2G034278 (Figure S11) exhibits MTHFR activity, it is possible that in *bm2* mutant plants GRMZM2G034278 may provide sufficient residual MTHFR activity to ensure survival but not normal accumulation of lignin.

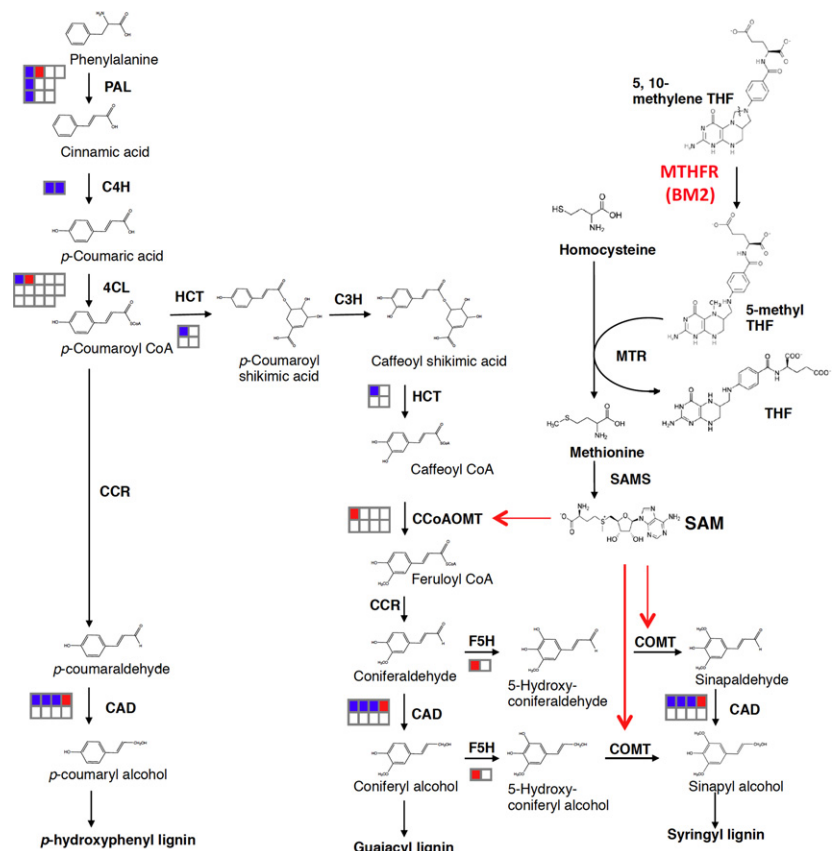
Role of the *bm2* gene in lignin biosynthesis

Consistent with previous reports (Vermerris and Boon, 2001; Marita *et al.*, 2003; Barriere *et al.*, 2004; Sattler *et al.*, 2010), we found that the *bm2* mutation reduces lignin accumulation (Table 1). We also found that lignin continues to accumulate after anthesis in both mutant and non-mutant sibling plants (Table 1).

The *bm2*-encoded MTHFR generates 5-methyltetrahydrofolate, which is used in the methylation of homocysteine to generate methionine (Goyette *et al.*, 1994; Vickers *et al.*, 2006). Subsequently, *S*-adenosyl-L-methionine (SAM) may be generated from methionine via the action of *S*-adenosyl-methionine synthetase. It has previously been shown that knockout of the gene encoding *S*-adenosylmethionine synthetase suppresses lignin biosynthesis (Shen *et al.*, 2002). Consistent with the fact that MTHFR is involved in the biosynthesis of SAM (Ravanel *et al.*, 1998), a number of SAM-dependent or SAM-related functional sub-groups (i.e. ethylene hormone metabolism, simple phenols and phenylpropanoids) are preferentially affected in the *bm2* mutant (Table S8) (Shen *et al.*, 2002). Two of these sub-groups (simple phenols and phenylpropanoids) are related to lignin biosynthesis. Indeed, many of the differentially expressed genes encode enzymes involved in lignin biosynthesis, such as PAL, HCT, ferulate-5-hydroxylase (F5H),

Figure 5. Relationship of *bm2* to the lignin biosynthetic pathway.

Modified biosynthetic pathway of monolignols (Bonawitz and Chapple, 2010; Vanholme *et al.*, 2010). The MTHFR (BM2) enzyme catalyzes the conversion of 5,10-methylenetetrahydrofolate to 5-methyltetrahydrofolate, which serves as a methyl donor to convert homocysteine to methionine. SAMs catalyzes the conversion of methionine to SAM, which is a methyl donor for CCoAOMT and COMT. The number of genes in families with at least one gene differentially expressed between *bm2* mutants and wild-type siblings is indicated by the number of rectangles. The number of significantly up- and down-regulated genes in *bm2* mutants relative to wild-type siblings are shown in blue and red, respectively. PAL, phenylalanine ammonia lyase; HCT, hydroxycinnamoyl CoA:shikimate hydroxycinnamoyl transferase; C4H, cinnamate 4-hydroxylase; 4CL, 4-coumarate:CoA ligase; C3H, *p*-coumarate 3-hydroxylase; CCR, cinnamoyl CoA reductase; CCoAOMT, caffeoyl CoA 3-*O*-methyltransferase; COMT, caffeic acid 3-*O*-methyltransferase; F5H, ferulate 5-hydroxylase; MTHFR, methylenetetrahydrofolate reductase; 5,10-methylene THF, 5,10-methylenetetrahydrofolate; 5-methyl THF, 5-methyltetrahydrofolate; THF, tetrahydrofolate; MTR, 5-methyltetrahydrofolate homocysteine methyltransferase; SAMS, *S*-adenosylmethionine synthetase; SAM, *S*-adenosyl-L-methionine.



CCoAOMT, CAD, C4H and 4CL (Table 2). Because SAM is consumed by both CCoAOMT and COMT (Ye *et al.*, 1994), alterations in the accumulation of SAM are expected to reduce the accumulation of both G- and S-lignin (Figure 5). Consistent with this expectation, our data confirm that the *bm2* mutant shows reduced accumulation of both G- and S-lignin (Vermerris and Boon, 2001; Marita *et al.*, 2003; Saballos *et al.*, 2009; Sattler *et al.*, 2010; Vermerris *et al.*, 2010).

EXPERIMENTAL PROCEDURES

Genetic stocks

Mutator-derived stocks originally obtained from Don Robertson (Iowa State University, Ames, IA, USA) have been maintained in the Schnable laboratory for many years. Various stocks carrying the *brown midrib2* reference allele (*bm2-ref*) were obtained from the Maize Genetics Cooperation Stock Center (maizecoop.cropsci.uiuc.edu/). These include stock numbers 90-896-4/895-2, 93-706-5/705, 93-705-2/706 and 2000-1695-7/1695-4 (Schnable Lab accession numbers Ac3247, Ac3246, Ac3245 and Ac3244, respectively).

The full-length *bm2* cDNA was PCR-amplified from each of these stocks using forward primer 5'-GTTATGAAGGTTATCGAG AAGATCCTGGAG-3' (which includes the start codon) and reverse primer 5'-TCAGATCTTGAAGGCAGCAAACAGG-3' (which includes the stop codon). The corresponding DNA fragments were then sequenced using the forward primers 5'-ATGAAGGTTATCGAGAA GATC-3', 5'-GATGCGATAACAAGGCGAGGG-3' and 5'-GCGCTTCA CAACTTCTGTC-3', and reverse primer 5'-GTAAAGGTGCAAAGTC TTAATGC-3'. Sequence analysis of full-length *bm2* cDNAs amplified from these stocks did not detect any polymorphisms among the various *bm2* mutant sources, suggesting that these stocks all carry the *bm2-ref* allele.

Mapping populations

A *bm2* mapping population was created by back-crossing homozygous *bm2-ref* mutant plants (Ac3247) as the male (pollen) parent onto the inbred line B73 (female parent) to generate F₁ seeds. Multiple F₁ plants were self-pollinated to create F₂ seeds that were used in the fine-mapping experiments. The F₂ seeds used in the BSR-Seq experiment were derived from a single F₁ plant.

Fine-scale mapping

DNA was extracted from leaf tissues sampled from 537 F₂ plants derived from a cross between B73 and *bm2-ref* homozygotes. SNPs identified during the BSR-Seq experiment (see below) and located within the mapping interval were sent to KBiosciences (now LGC Genomics, www.lgcgenomics.com) for KASPar SNP primer design (www.lgcgenomics.com/genotyping/kasp-genotyping-reagents/kasp-assays-kbd-kod/?id=69). The 537 individuals from the F₂ mapping population were individually subjected to KASPar-based SNP genotyping (Cuppen, 2007) using the flanking SNP markers *bm2*-290599983 and *bm2*-291111263 (Table S2) to identify recombinants. Additional SNPs were used to similarly genotype recombinant plants to more precisely define the *bm2* mapping interval.

Isolation of RNA for two independent RNA-Seq experiments

For RNA-Seq experiment #1, F₂ seeds from a single heterozygous individual (genotype *Bm2/bm2-ref*; Maize Genetics Cooperation

Stock Center, stock center ID 90-896-4/895-2) (Schnable Lab accession number Ac3247) were grown in a greenhouse under 15 h light/9 h dark (27°C/24°C, 30% humidity). The light intensity was approximately 650–800 μmol m⁻² s⁻¹. Leaf tissue samples were collected from 53 26-day-old phenotypically mutant plants and 53 phenotypically non-mutant plants. A 5.5 cm segment of leaf tissue (measured from the stem) was collected from the second youngest leaf from each individual plant. Corresponding midrib tissue samples were pooled for RNA extraction. RNA was extracted from tissues using RNeasy mini kits (Qiagen, www.qiagen.com) with DNase I treatment according to the manufacturer's instructions. RNA quality was analyzed using a Bioanalyzer 2100 RNA nanochip (Agilent Technologies, www.agilent.com) according to the manufacturer's instructions. RNA-Seq libraries were constructed using an Illumina RNA-Seq sample preparation kit according to the manufacturer's instructions (www.illumina.com). The libraries were sequenced on an Illumina Genome Analyzer II, generating approximately 75 bp reads.

Subsequently, a second RNA-Seq experiment (#2) was performed. F₂ seeds from a heterozygous individual (genotype *Bm2/bm2-ref*) were grown. A 5.5 cm segment of leaf tissue (measured from the stem) was collected from the second youngest leaf of each 38-day-old plant individual. Two biological replicates of mutant and wild-type sibling tissue samples were collected. In each replication, the midribs of leaf samples from 20 mutant and 20 wild-type individuals were pooled separately for RNA extraction. This RNA-Seq experiment was similar to the first RNA-Seq experiment except that: (i) midribs were collected from 38-day-old plants rather than 26-day-old plants, (ii) midribs from 20 individuals were pooled in each sample, and (iii) 101 bp paired-end reads were generated on an Illumina HiSeq2000 instrument.

Trimming and mapping of RNA-Seq reads

Raw reads were subjected to quality checking and trimming to remove low-quality bases using a custom written trimming script (Liu *et al.*, 2012). Trimming parameters were set similarly to the defaults for *Lucy2* trimming software (Li and Chou, 2004). Trimmed reads were aligned to the B73 reference genome (B73Ref2) using GSNAP (Wu and Nacu, 2010), and uniquely mapped reads (allowing two mismatches every 36 bp, and 3 bp tails per 75 bp) were used for subsequent analyses. The read depth of each gene of the filtered gene set (ZmB73_5b_FGS, see ftp.maizesequence.org/current/filtered-set/ for files) was computed based on the coordinates of mapped and annotated locations of genes in the B73 reference genome.

Mapping *bm2* via BSR-Seq

Reads from the first RNA-Seq experiment were used to map *bm2* via BSR-Seq (Liu *et al.*, 2012). After aligning trimmed reads from the *bm2* and wild-type sibling pools, SNPs were discovered and quantified at each SNP site in each sample pool (mutant and wild-type). Finally, a Bayesian-based bulked segregant analysis (BSR-Seq), which accounts for biological/technical variation, was used to map the *bm2* gene (Liu *et al.*, 2012).

Analysis of RNA-Seq experiment #1

Normalization was performed using a method that corrects for biases introduced by RNA composition and differences in the total numbers of uniquely mapped reads in each sample (Robinson and Oshlack, 2010). Normalized read counts were used to calculate fold changes and statistical significance. Fisher's exact test was used to test the null hypothesis that the expression level of a given gene is not different between the two samples. Because the

first experiment did not include biological replication, statistically significant variation may be a consequence of either biological or technical variation in gene expression between a pair of samples. Genes identified as candidates for differential expression were further filtered using an absolute \log_2 fold change >1 and a q value cut-off of 0.00001 to account for multiple testing (Benjamini and Hochberg, 1995). These genes are referred to as 'significantly differentially expressed' and were functionally classified using the MapMan functional classification system (Thimm *et al.*, 2004).

Analysis of the RNA-Seq experiment #2

Genes with at least one uniquely mapped read across samples and at least two samples with positive read counts were tested for differential expression between the *bm2* mutant and wild-type sibling using the R package QuasiSeq (<http://cran.r-project.org/web/packages/QuasiSeq>). The negative binomial QLSpline method implemented in the QuasiSeq package was used to calculate a P value for each gene (Lund *et al.*, 2012). The 0.75 quantile of reads from each sample was used as the normalization factor (Bullard *et al.*, 2010). A multiple test controlling approach (Nettleton *et al.*, 2006) was used to estimate the number of genes with true null hypotheses among all genes tested, and this estimate was used to convert the P values to q values (Storey, 2002). To obtain approximate control of the false discovery rate at 5%, genes with q values no larger than 0.05 were considered differentially expressed.

Enrichment analysis of significantly differentially expressed genes in RNA-Seq experiment #2

Functional annotation of maize genes was downloaded from <http://mapman.gabipd.org/>. Similar to the PageMan enrichment analysis (Usadel *et al.*, 2006), Fisher's exact test was used to test the null hypothesis of no enrichment of a certain functional group of genes in the set of differentially expressed genes. To avoid dependency of functional groups across various layers of annotation, which introduces complexity during multiple test control, we performed enrichment analysis for each annotation layer separately.

Direct transposon (*Mu*) tagging of *bm2*

Additional *bm2* alleles were isolated from a forward genetic screen of approximately 147 500 individuals generated by crossing active *Mu* stocks (genotype of *Bm2/Bm2; Mu*) as females with males homozygous for the *bm2-ref* allele. The male parent in this cross was derived from a mixture of the four stocks obtained from the Maize Genetics Cooperation Stock Center. A *Mutator* transposon-specific primer (MuTIR) and *bm2* gene-specific primers were used to analyze individuals that exhibited a brown midrib phenotype to identify *Mutator* insertion alleles in the *bm2* gene (*bm2-Mu*) (Figure S1).

Measurement of *bm2* expression via quantitative RT-PCR

Quantitative RT-PCR was performed on two biological replicates of 11 homozygous *bm2-Mu* lines and B73 (described above). Each biological replicate represents a pool of midrib tissue collected from 2 to 4 individual 1-month-old plants. Collection of midrib tissue was performed as described above. RNA was isolated and purified using RNeasy mini kits (Qiagen), before reverse transcription into cDNA using SuperScript™ III reverse transcriptase (Invitrogen, www.lifetechnologies.com) according to the manufacturer's instructions. qRT-PCR was performed using ABsolute™ qPCR SYBR® Green Mix (Thermo Scientific) on Roche Lightcycler 480 quantitative PCR system (Roche, www.nimblegen.com).

Quantitative RT-PCR data were analyzed using Roche LIGHTCYCLER 480 analysis software. The following PCR conditions were used to detect transcript levels: 2 min at 50°C, 10 min at 95°C (pre-denaturation), 40 cycles of 15 sec at 95°C/1 min at 60°C (denaturation/annealing/amplification), with a temperature of 60°C for the melting curve start temperature. C_t values were calculated using the second derivative maximum method with baseline-corrected, 6-carboxy-X-rhodamine (ROX)-normalized parameters (for details, see LightCycler 480 Operator's Manual accessible at icob.sinica.edu.tw/pubweb/Core%20Facilities/Data/R401-core/LightCycler480%20II_Manual_V1.5.pdf). One plate was analyzed for each group of biological replicates. Each sample was analyzed using *bm2* and glyceraldehyde-3-phosphate dehydrogenase gene primers separately. Three technical replicates were analyzed for each reaction, and the mean C_t value of these three replicates was used for further data analysis. Standard curves for quantification were constructed based on four fivefold serial dilutions of B73 DNA with *bm2* or glyceraldehyde-3-phosphate dehydrogenase gene primers. Samples were normalized using glyceraldehyde-3-phosphate dehydrogenase gene. The following primers were used for detection of the corresponding mRNAs: *bm2* forward primer 5'-ATGATGGGTTCCGAGAATCA-3' and reverse primer 5'-GGATGTTCCACCTATATTCTGG-3'; glyceraldehyde-3-phosphate dehydrogenase gene forward primer 5'-GCTTCTCATGGATGGTTGCT-3' and reverse primer 5'-CAGGAAGGGAAGCAAAGTG-3'.

Phloroglucinol staining and light microscopy

Midrib, stem and root tissue samples were hand-sectioned to a thickness of 200 μm using double-edge razors (Wilkinson Sword, www.wilkinsonsword.co.uk/), and stored in sterile distilled water for 2 h or less until sample sectioning was completed. Phloroglucinol staining was performed as described previously (Nakano and Meshitsuka, 1992). Briefly, phloroglucinol (Sigma-Aldrich, www.sigmaaldrich.com) was dissolved in 95% ethanol (Decon Laboratories Inc., www.deconlabs.com) to form a 2% stock solution. Immediately before use, concentrated hydrochloric acid (33% v/v) was mixed with the stock solution to form the phloroglucinol staining solution, which was directly applied to samples. Maize tissue samples were placed on glass slides (Thermo Fisher Scientific, www.thermofisher.com). Excess solution was removed from the glass slides using Kimwipes (Kimberly-Clark, www.kimberly-clark.com). Phloroglucinol stain (300 μl) was applied to the samples for 30 sec, with a cover glass (Corning, www.corning.com) on top. Additional phloroglucinol staining solution was added to the sample until it was fully covered by solution. Light images were captured using a Spot RT slider camera (Diagnostic Instruments Inc., www.spotimaging.com/) on a Nikon Eclipse E800 microscope (www.nikoninstruments.com/) at 20 x magnification, and analyzed using SPOT version 4.0.6 software (Diagnostic Instruments Inc.).

Actinomycin D treatment

A small circular piece of the 2nd youngest leaf (approximately 0.02 g) of various genotypes was obtained using a hole punch. The samples were incubated in water (negative control), actinomycin D (50 $\mu\text{g ml}^{-1}$) or DMSO (10 $\mu\text{l ml}^{-1}$, solvent control) for 12 h at room temperature. Solutions were changed every 4 h. The samples were then subjected to RNA purification and RT-PCR.

Yeast complementation assay

Saccharomyces cerevisiae strains of the following genotypes were kindly provided by Warren D. Kruger (Division of Population Science, Fox Chase Cancer Center, Philadelphia, PA, USA) (Shan *et al.*, 1999): W303-1A (wild-type, also labeled *MET11: Mata*,

ade2-1, can1-100, ura3-1, leu2-3, 112, trp1-1, his3-11,15 and XSY3-1A (*Met11* knockout strain, also labeled *met11: Mata, ade2-1, can1-100, ura3-1, leu2-3,112, trp1-1, his3-11,15, met11Δ::TRP1*). The galactose-inducible human MTHFR expression plasmid pHMTHFR (which contains the human MTHFR-encoding cDNA inserted in pHMV2.1 from Shan *et al.* 1999) was also provided by Warren D. Kruger (Shan *et al.*, 1999). To obtain wild-type maize *bm2* cDNA, RNA was extracted from wild-type maize (B73), and then subjected to RT-PCR. The full-length (1782 bp) wild-type maize *bm2* cDNA was first amplified from B73 cDNA using forward primer 5'-GTTATGAAGGTTAT CGAGAAGATCCTGGAG-3' (including the start codon) and reverse primer 5'-TCAGATCTT GAAGGCAGCAAACAGG-3' (including the stop codon). The fragment was cloned into the galactose-inducible expression plasmid pYES2.1/V5-His-TOPO using a pYES2.1 TOPO® TA expression kit (both supplied by Life Technologies, www.lifetechnologies.com/us/en/home.html). Plasmids were transformed into yeast using the S.c. EasyComp™ transformation kit (Invitrogen). The cloned fragment was then sequenced using forward primers 5'-ATGAAGTTATCGAGAAGATC-3', 5'-GATGCGATACAAGCGAGGG-3' and 5'-GCGTTCACAACTTCTGTC-3', and reverse primer 5'-GTAAAGGTGCAAAGTCTTAATGC-3'. To test the growth of the transformed yeast for complementation, yeast cells were inoculated on plates containing SD glucose -Met (control) or SD galactose -Met (to induce expression of the insert at the plasmid), which were then incubated at 30°C for 3 days. DIFCO brand SD base was supplied by BD Biosciences (www.bdbiosciences.com) and dropout supplements by Clontech (www.clontech.com).

Klason lignin

Entire non-mutant sibling and *bm2-ref* mutant whole stalks were destructively sampled for Klason lignin analysis post-anthesis (approximately 2 months after planting) and post-senescence (approximately 5 months after planting) from field-grown F₂ plants derived from a hybrid resulting from the cross of a *bm2-ref* mutant with B73. Stalks were cut at the first above-ground node, and leaves, tassels and ears were removed before air-drying for several weeks. After drying, stalks were processed in a Wiley mill (Arthur H. Thomas Co., www.ahthomas.com) with a 1 mm filter, and the ground stover was further processed for 10 sec in a coffee grinder.

Klason lignin was determined according to the protocol 'Determination of Acid-Insoluble Lignin in Biomass' released by the Department of Energy's National Renewable Energy Laboratory in 1995 (accessible at infohouse.p2ric.org/ref/40/39182.pdf). Standard acid hydrolysis was performed on 300 mg stalk stover in 72% H₂SO₄ at 30°C for 2 h and in 4% H₂SO₄ at 121°C in an autoclave for 1 h. Acid-insoluble lignin was vacuum-filtered, dried and weighed. Total Klason lignin was determined by firing the solid for 3 h at 575°C and subtracting the resulting ash weight from the lignin weight. Grams of Klason lignin per gram of dry weight was calculated by dividing the total Klason lignin weight by the initial weight of dry matter used.

Thioacidolysis

Thioacidolysis of maize stover was performed as described previously (Robinson and Mansfield, 2009). The stover used for thioacidolysis came from the same plants as that used for Klason lignin analysis. For each sample, approximately 300 mg ground stover was extracted in 1 ml of a 35:4:1 solution of dioxane, ethanethiol and boron trifluoride for 4 h at 100°C. After adjusting the pH with 500 µl of 0.4 M NaHCO₃, 2 ml H₂O, 200 µl of a 0.5 mg ml⁻¹ tetracosane standard and 0.5 ml methylene chloride

were added to each sample. Samples were then filtered over anhydrous Na₂SO₄, vacuum-dried and resuspended in 500 µl methylene chloride. A 40 µl aliquot of sample was derivatized for 2 h using 40 µl pyridine and 200 µl *N,O*-bis(trimethylsilyl)trifluoroacetamide. After derivatization, samples were dried again under a nitrogen evaporator and resuspended in 500 µl chloroform before analysis by GC-MS.

GC-MS was performed on an Agilent Technologies model 7890A instrument coupled to a model 5975C mass selective detector with autosampler, split-less injector and an Agilent HP-5MS capillary column (30 m length × 0.25 mm internal diameter, 0.25 µm particle size). The electron ionization voltage and interface temperature were set to 70 eV and 280°C, respectively. The injection volume was set at 1 µl, with helium as the carrier gas and a constant flow rate of 1 ml min⁻¹. The initial temperature was set to 130°C, hold 3 min, ramp temperature 20°C min⁻¹ to 240°C, ramp temperature 5°C min⁻¹ to a final temperature of 320°C, which was held for 4 min.

Using reconstructed ion chromatograms, S-lignin monomers were detected at *m/z* 299 and 135 (molecular ion of 448), while G-lignin monomers were detected at *m/z* 269 and 135 (molecular ion of 418). Like other grasses, maize accumulates very low amounts of H-lignin. The minor peaks associated with H-lignin were not detected in this experiment. Tetracosane was detected at *m/z* 57 (Rolando *et al.*, 1992). The amount of S- and G-lignin (µmol) was calculated by dividing the area of the S- or G-lignin peaks, respectively, by the tetracosane peak area, and multiplying by the number of moles of tetracosane standard added. The number of µmoles of S- and G-lignin was then divided by the total weight of tissue used in the sample preparation.

Phylogenetic analysis of BM2

Orthologs of maize BM2 were identified using the National Center for Biotechnology Information Protein BLAST algorithm (blast.ncbi.nlm.nih.gov/Blast.cgi) on the maize *bm2* protein sequence. All parameters were default except the 'expect' threshold, which was set to 0.00001. The resulting 2099 non-redundant protein sequences were narrowed down to 18 land-plant RefSeqs with greater than 40% identity and coverage of the maize protein sequence. Because these proteins vary in length, a phylogenetic tree was constructed using only the conserved region of MTHFR, which corresponds to residues 167–350 of the BM2 protein sequence. The tree was constructed in Jalview (www.jalview.org) via Blosum62 (www.ncbi.nlm.nih.gov/Class/FieldGuide/BLOSUM62.txt) neighbor joining using a consensus sequence constructed from the 18 RefSeqs.

Expression pattern of *bm2*

The expression pattern for maize *bm2* was visualized using the online tool qTeller (qTeller.com). The RNA-Seq data provided by qTeller (both published and unpublished) comes from a variety of sources throughout the maize community. More information on the origin of the datasets and in-house analysis of the data may be found on the qTeller website.

ACKNOWLEDGEMENTS

We thank Lisa Coffey for maintaining stocks, performing the *bm2* mutant screen, and generating mapping populations, Marianne Smith for technical support with phloroglucinol staining and microscopy, Warren D. Kruger (Division of Population Science, Fox Chase Cancer Center, Philadelphia, PA, USA) for providing yeast strains W303-1A and XSY3-1A and the *phMTHFR* plasmid,

and Ann Perera and Zhihong Song (W.M. Keck Metabolomics Research Laboratory, Iowa State University, Ames, IA, USA) for their expertise in GC-MS.

SUPPORTING INFORMATION

Additional Supporting Information may be found in the online version of this article.

Figure S1. Identification of *Mutator* insertion alleles in the *bm2* locus.

Figure S2. *bm2* encodes a putative MTHFR.

Figure S3. Histochemical staining of lignin in tissue sections from wild-type and the *bm2-Mu* mutant.

Figure S4. Polymorphisms in the *bm2-ref* allele compared to the *Bm2-B73* wild-type allele.

Figure S5. Alignment of deduced amino acid sequences of the *Bm2* gene with the sequence of *MET11* from *Saccharomyces cerevisiae*.

Figure S6. Histogram of *P* values for differential expression tests.

Figure S7. Volcano plot from RNA-Seq.

Figure S8. MA plot from RNA-Seq.

Figure S9. Comparison of fold changes between two RNA-Seq experiments on 369 differentially expressed genes.

Figure S10. Overview of differential expression in the metabolic pathway.

Figure S11. Phylogenetic tree of the maize MTHFR conserved region.

Figure S12. qTeller expression pattern of *bm2*.

Table S1. Genes in the 2 Mb interval as inferred from BSR-Seq.

Table S2. Fine-mapping primer sequences for the KASPar assay.

Table S3. The 47 genes in the 0.51 MB *bm2* interval (working gene set).

Table S4. The eight genes in the 0.51 MB *bm2* interval (filtered gene set).

Table S5. Trimming and alignment summary for RNA-Seq experiment #1.

Table S6. Read trimming summary for RNA-Seq experiment #2.

Table S7. Alignment summary for RNA-Seq experiment #2.

Table S8. Overall represented pathways (MapMan).

Table S9. Genes in the phenylpropanoid pathway that did not exhibit significantly differential expression.

Appendix S1. Differential expression between *bm2* and the wild-type.

REFERENCES

Amir, R. (2010) Current understanding of the factors regulating methionine content in vegetative tissues of higher plants. *Amino Acids*, **39**, 917–931.

Barrière, Y., Chavigneau, H., Delaunay, S., Courtial, A., Bosio, M., Lassagne, H., Derory, J., Lapierre, C., Méchin, V. and Tatout, C. (2013) Different mutations in the *ZmCAD2* gene underlie the maize brown-midrib1 (*bm1*) phenotype with similar effects on lignin characteristics and have potential interest for bioenergy production. *Maydica*, **58**.

Barrière, Y., Ralph, J., Mechin, V., Guillaumie, S., Grabber, J.H., Argillier, O., Chabbert, B. and Lapierre, C. (2004) Genetic and molecular basis of grass cell wall biosynthesis and degradability. II. Lessons from brown-midrib mutants. *C. R. Biol.*, **327**, 847–860.

Barrière, Y., Riboulet, C., Méchin, V., Maltese, S., Pichon, M., Cardinal, A., Lapierre, C., Lübberstedt, T. and Martinant, J.-P. (2007) Genetics and genomics of lignification in grass cell walls based on maize as model species. In *Genes, Genomes and Genomics* (Teixeira da Silva, J.A., and Shima, K., eds.). Middlesex: Global Science Books, pp. 133–156.

Benjamini, Y. and Hochberg, Y. (1995) Controlling the false discovery rate: a practical and powerful approach to multiple testing. *J. R. Stat. Soc. B*, **57**, 289–300.

Bonawitz, N.D. and Chapple, C. (2010) The genetics of lignin biosynthesis: connecting genotype to phenotype. *Annu. Rev. Genet.*, **44**, 337–363.

Bullard, J.H., Purdom, E., Hansen, K.D. and Dudoit, S. (2010) Evaluation of statistical methods for normalization and differential expression in mRNA-Seq experiments. *BMC Bioinformatics*, **11**, 94.

Chen, Y., Liu, H., Ali, F., Scott, M.P., Ji, Q., Frei, U.K. and Lübberstedt, T. (2012) Genetic and physical fine mapping of the novel brown midrib gene *bm6* in maize (*Zea mays L.*) to a 180 kb region on chromosome 2. *Theor Appl Genet*, **125**, 1223–1235.

Cherney, J.H., Cherney, D.J.R., Akin, D.E. and Axtell, J.D. (1991) Potential of brown-midrib, low-lignin mutants for improving forage. *Adv. Agron.*, **46**, 157–198.

Cuppen, E. (2007) Genotyping by allele-specific amplification (KASPar). *CSH Protoc.*, **2007**, pdb.prot4841.

Dietrich, C.R., Cui, F., Packila, M.L., Li, J., Ashlock, D.A., Nikolau, B.J. and Schnable, P.S. (2002) Maize Mu transposons are targeted to the 5' untranslated region of the *gl8* gene and sequences flanking Mu target-site duplications exhibit nonrandom nucleotide composition throughout the genome. *Genetics*, **160**, 697–716.

Doebley, J.F., Gaut, B.S. and Smith, B.D. (2006) The molecular genetics of crop domestication. *Cell*, **127**, 1309–1321.

Fu, C., Mielenz, J.R., Xiao, X. et al. (2011) Genetic manipulation of lignin reduces recalcitrance and improves ethanol production from switchgrass. *Proc. Natl Acad. Sci. USA*, **108**, 3803–3808.

Goyette, P., Sumner, J.S., Milos, R., Duncan, A.M., Rosenblatt, D.S., Matthews, R.G. and Rozen, R. (1994) Human methylenetetrahydrofolate reductase: isolation of cDNA, mapping and mutation identification. *Nat. Genet.*, **7**, 195–200.

Grand, C.P., Parmentier, P., Boudet, A. and Boudet, A.M. (1985) Comparison of lignins and enzymes involved in lignification in normal and brown midrib (*bm3*) mutant corn seedlings. *Physiol. Veg.*, **23**, 905–911.

Gutierrez, R.A., MacIntosh, G.C. and Green, P.J. (1999) Current perspectives on mRNA stability in plants: multiple levels and mechanisms of control. *Trends Plant Sci.*, **4**, 429–438.

Halpin, C., Holt, K., Chojecki, J., Oliver, D., Chabbert, B., Monties, B., Edwards, K., Barakate, A. and Foxon, G.A. (1998) *Brown-midrib maize (bm1)* - a mutation affecting the cinnamyl alcohol dehydrogenase gene. *Plant J*, **14**, 545–553.

Jiang, N., Ferguson, A.A., Slotkin, R.K. and Lisch, D. (2011) Pack-Mutator-like transposable elements (Pack-MULEs) induce directional modification of genes through biased insertion and DNA acquisition. *Proc. Natl Acad. Sci. USA*, **108**, 1537–1542.

Jorgenson, L.R. (1931) Brown midrib in maize and its linkage relations. *J. Am. Soc. Agron.*, **23**, 549–557.

Jung, H.G. and Vogel, K.P. (1986) Influence of lignin on digestibility of forage cell wall material. *J. Anim. Sci.*, **62**, 1703–1712.

Lawrence, C.J., Seigfried, T.E. and Brendel, V. (2005) The maize genetics and genomics database. The community resource for access to diverse maize data. *Plant Physiol.*, **138**, 55–58.

Lewis, N.G. and Yamamoto, E. (1990) Lignin: occurrence, biogenesis and biodegradation. *Annu. Rev. Plant Physiol. Plant Mol. Biol.*, **41**, 455–496.

Li, S. and Chou, H.H. (2004) LUCY2: an interactive DNA sequence quality trimming and vector removal tool. *Bioinformatics*, **20**, 2865–2866.

Liu, S., Yeh, C.T., Tang, H.M., Nettleton, D. and Schnable, P.S. (2012) Gene mapping via bulked segregant RNA-Seq (BSR-Seq). *PLoS ONE*, **7**, e36406.

Lund, S.P., Nettleton, D., McCarthy, D.J. and Smyth, G.K. (2012) Detecting differential expression in RNA-sequence data using quasi-likelihood with shrunken dispersion estimates. *Stat. Appl. Genet. Mol. Biol.*, **11**, 1–42. doi:10.1515/1544-6115.1826.

Marita, J.M., Vermerris, W., Ralph, J. and Hatfield, R.D. (2003) Variations in the cell wall composition of maize brown midrib mutants. *J. Agric. Food Chem.*, **51**, 1313–1321.

Millevoi, S. and Vagner, S. (2010) Molecular mechanisms of eukaryotic pre-mRNA 3' end processing regulation. *Nucleic Acids Res.*, **38**, 2757–2774.

Nakano, J. and Meshitsuka, G. (1992) The detection of lignin. In *Methods in Lignin Chemistry* (Lin, S.Y. and Dence, C.W., eds). Berlin: Springer-Verlag, pp. 23–32.

- Nettleton, D., Hwang, J.T.G., Caldo, R.A. and Wise, R.P. (2006) Estimating the number of true null hypotheses from a histogram of *p* values. *J. Agric. Biol. Environ. Stat.*, **11**, 337–356.
- Neuffer, M.G., Jones, L. and Zuber, M.S. (1968) *The Mutants of Maize; A Pictorial Survey in Color of the Usable Mutant Genes in Maize with Gene Symbols and Linkage Map Positions*. Madison, WI: Crop Science Society of America.
- Penning, B.W., Hunter, C.T. III, Tayengwa, R. *et al.* (2009) Genetic resources for maize cell wall biology. *Plant Physiol.*, **151**, 1703–1728.
- Quiroga, M., Guerrero, C., Botella, M.A., Barcelo, A., Amaya, I., Medina, M.I., Alonso, F.J., de Forchetti, S.M., Tigier, H. and Valpuesta, V. (2000) A tomato peroxidase involved in the synthesis of lignin and suberin. *Plant Physiol.*, **122**, 1119–1127.
- Ragauskas, A.J., Williams, C.K., Davison, B.H. *et al.* (2006) The path forward for biofuels and biomaterials. *Science*, **311**, 484–489.
- Ravanel, S., Gakiere, B., Job, D. and Douce, R. (1998) The specific features of methionine biosynthesis and metabolism in plants. *Proc. Natl Acad. Sci. USA*, **95**, 7805–7812.
- Robinson, A.R. and Mansfield, S.D. (2009) Rapid analysis of poplar lignin monomer composition by a streamlined thioacidolysis procedure and near-infrared reflectance-based prediction modeling. *Plant J.*, **58**, 706–714.
- Robinson, M.D. and Oshlack, A. (2010) A scaling normalization method for differential expression analysis of RNA-seq data. *Genome Biol.*, **11**, R25.
- Roje, S., Wang, H., McNeil, S.D., Raymond, R.K., Appling, D.R., Shachar-Hill, Y., Bohnert, H.J. and Hanson, A.D. (1999) Isolation, characterization, and functional expression of cDNAs encoding NADH-dependent methylenetetrahydrofolate reductase from higher plants. *J. Biol. Chem.*, **274**, 36089–36096.
- Rolando, C., Monties, B. and Lapierre, C. (1992) Thioacidolysis. In *Methods in Lignin Chemistry* (Lin, S. and Dence, C., eds). Berlin: Springer-Verlag, pp. 334–349.
- Saballos, A., Ejeta, G., Sanchez, E., Kang, C. and Vermerris, W. (2009) A genome-wide analysis of the cinnamyl alcohol dehydrogenase family in sorghum [*Sorghum bicolor* (L.) Moench] identifies *SbCAD2* as the *Brown midrib6* gene. *Genetics*, **181**, 783–795.
- Sarkanen, K.V. and Ludwig, C.H. (1971) Definition and nomenclature. In *Lignins: Occurrence, Formation, Structure and Reactions* (Sarkanen, K.V. and Ludwig, C.H., eds). New York: Wiley-Interscience, pp. 1–17.
- Sattler, S.E., Funnell-Harris, D.L. and Pedersen, J.F. (2010) Brown midrib mutations and their importance to the utilization of maize, sorghum, and pearl millet lignocellulosic tissues. *Plant Sci.*, **178**, 229–238.
- Sawicki, S.G. and Godman, G.C. (1972) On the recovery of transcription after inhibition by actinomycin D. *J. Cell Biol.*, **55**, 299–309.
- Schnable, P.S., Ware, D., Fulton, R.S. *et al.* (2009) The B73 maize genome: complexity, diversity, and dynamics. *Science*, **326**, 1112–1115.
- Shan, X., Wang, L., Hoffmaster, R. and Kruger, W.D. (1999) Functional characterization of human methylenetetrahydrofolate reductase in *Saccharomyces cerevisiae*. *J. Biol. Chem.*, **274**, 32613–32618.
- Shen, B., Li, C. and Tarczynski, M.C. (2002) High free-methionine and decreased lignin content result from a mutation in the Arabidopsis S-adenosyl-L-methionine synthetase 3 gene. *Plant J.*, **29**, 371–380.
- Storey, J.D. (2002) A direct approach to false discovery rates. *J. R. Stat. Soc. B*, **64**, 479–498.
- Tamasloukht, B., Wong Quai Lam, M.S., Martinez, Y. *et al.* (2011) Characterization of a cinnamoyl-CoA reductase 1 (CCR1) mutant in maize: effects on lignification, fibre development, and global gene expression. *J. Exp. Bot.*, **62**, 3837–3848.
- Tang, H., Sezen, U. and Paterson, A.H. (2010) Domestication and plant genomes. *Curr. Opin. Plant Biol.*, **13**, 160–166.
- Thimm, O., Blasing, O., Gibon, Y., Nagel, A., Meyer, S., Kruger, P., Selbig, J., Muller, L.A., Rhee, S.Y. and Stitt, M. (2004) MAPMAN: a user-driven tool to display genomics data sets onto diagrams of metabolic pathways and other biological processes. *Plant J.*, **37**, 914–939.
- Usadel, B., Nagel, A., Steinhauser, D. *et al.* (2006) PageMan: an interactive ontology tool to generate, display, and annotate overview graphs for profiling experiments. *BMC Bioinformatics*, **7**, 535.
- Vanholme, R., Demedts, B., Morreel, K., Ralph, J. and Boerjan, W. (2010) Lignin biosynthesis and structure. *Plant Physiol.*, **153**, 895–905.
- Vermerris, W. and Boon, J.J. (2001) Tissue-specific patterns of lignification are disturbed in the *brown midrib2* mutant of maize (*Zea mays* L.). *J. Agric. Food Chem.*, **49**, 721–728.
- Vermerris, W., Sherman, D.M. and McIntyre, L.M. (2010) Phenotypic plasticity in cell walls of maize brown midrib mutants is limited by lignin composition. *J. Exp. Bot.*, **61**, 2479–2490.
- Vickers, T.J., Orsomando, G., de la Garza, R.D., Scott, D.A., Kang, S.O., Hanson, A.D. and Beverley, S.M. (2006) Biochemical and genetic analysis of methylenetetrahydrofolate reductase in *Leishmania* metabolism and virulence. *J. Biol. Chem.*, **281**, 38150–38158.
- Vignols, F., Rigau, J., Torres, M.A., Capellades, M. and Puigdomenech, P. (1995) The *brown midrib3* (*bm3*) mutation in maize occurs in the gene encoding caffeic acid O-methyltransferase. *Plant Cell*, **7**, 407–416.
- Wardrop, A.B. (1971) *Lignins: Occurrence, Formation, Structure and Reactions*. New York: Wiley-Interscience.
- Whetten, R. and Sederoff, R. (1995) Lignin biosynthesis. *Plant Cell*, **7**, 1001–1013.
- Wu, T.D. and Nacu, S. (2010) Fast and SNP-tolerant detection of complex variants and splicing in short reads. *Bioinformatics*, **26**, 873–881.
- Ye, Z.H., Kneusel, R.E., Matern, U. and Varner, J.E. (1994) An alternative methylation pathway in lignin biosynthesis in *Zinnia*. *Plant Cell*, **6**, 1427–1439.